Supporting Information

Metal Ion Sensing Using ion Chemical Exchange Saturation Transfer-^{19}F Magnetic Resonance Imaging

Amnon Bar-Shir[†,‡], Assaf A. Gilad[†,‡,§], Kannie W.Y. Chan[†,§], Guanshu Liu[†,§], Peter C.M. van Zijl[†,§], Jeff W.M. Bulte[†,‡,§,||,^,#] * and Michael T. McMahon[†,§,*].

†Russell H. Morgan Department of Radiology and Radiological Science, The Johns Hopkins Hospital, Baltimore, Maryland 21287, United States

‡Cellular Imaging Section and Vascular Biology Program, Institute for Cell Engineering, The Johns Hopkins University School of Medicine, Baltimore, Maryland 21205, United States

[§]F. M. Kirby Research Center for Functional Brain Imaging, Kennedy Krieger Institute, Baltimore, Maryland 21205, United States

||Department of Biomedical Engineering, The Johns Hopkins University School of Medicine, Baltimore, Maryland 21205, United States

⊥Department of Chemical and Biomolecular Engineering, Johns Hopkins University, Baltimore, Maryland 21218, United States

#Department of Oncology, Johns Hopkins University School of Medicine, Baltimore, Maryland 21205, United States

Supporting Information

Experimental Section

5F-BAPTA (5,5'-difluoro BAPTA): The difluoro derivative of the tetra potassium salt of [1,2,-bis(o-aminophenoxy)ethane-N,N,-N',N', tetra-acetic acid], 5F-BAPTA, was purchased from Biotium, Inc. (Hayward, CA, USA).

Sample preparation: 5F-BAPTA was dissolved in Hepes buffer (40 mM) to a final concentration of 10 mM and the pH was adjusted to the following values: 5.6, 6.0, 6.4, 6.8, 7.0, 7.2, and 7.6. Stock 10 mM solutions of $CaCl_2$, $MgCl_2$, and $ZnCl_2$ were prepared in 40 mM Hepes buffer. Five μL of the stock solution was added to 1 mL of 10 mM 5F-BAPTA resulting in a 200:1 ratio (10 mM: 50 μM) between the free 5F-BAPTA and the M^{2+} ion following by a pH adjustment. One mL of each sample (with adjusted pH) was transferred into a 8 mm NMR tube within a 25 mm NMR tube in order to center the sample in the coil for the MRI experiments.

^{19}F NMR experiments: ^{19}F-NMR spectra were acquired with 11.7 T NMR scanner (Bruker) with a dedicated ^{19}F coil (470 MHz). Samples contained 5F-BAPTA (5.0 mM) M^{2+} (Ca^{2+}, Mg^{2+} or Zn^{2+}, 0.5 mM), 5-Fluoro-Cytosine (5-FC, 0.5 mM) and D_2O (10%) that was used for signal lock. 5FC was assigned as an internal reference with a fixed frequency of -47.0 ppm. Interestingly, the data show that the frequency of free 5F-BAPTA is affected by pH, while that of bound 5F-BAPTA is not. Experiments were run at 25, 31, and 37ºC to assess the effect of temperature on the frequency offsets of free 5F-BAPTA and [Ca^{2+}-5F-BAPTA]. At 37ºC, additional tubes containing K^+ (120 mM) or K^+

+ Mg^{2+} (120 mM + 1 mM, respectively) were also tested to determine the effect on Δω of ions fast exchanging with 5F-BAPTA.

MRI: MRI experiments were performed on a vertical 16.4 T scanner (Bruker Avance system) at 37ºC. A 25 mm birdcage radiofrequency coil was used to acquire both ^{1}H and ^{19}F MR images by sweeping the coil frequency from proton (700 MHz) to fluorine (658.8 MHz) frequency.

^{1}H-MRI: A RARE sequence was used to acquire the ^{1}H-MR images with the following parameters: TR/TE=5,000/7.7 ms, RARE factor=8, 1 mm slice thickness, FOV=4×4 cm, matrix size=128×128, resolution=0.3125×0.3125 mm, and 1 average (NA=1).

^{19}F-iCEST experiments: A modified RARE sequence (TR/TE=4,000/3.4 ms, RARE factor=4, 10 mm slice thickness, FOV=4×4 cm, matrix size=32×32, resolution=1.25×1.25 mm, and NA=8) including a magnetization transfer (MT) module (B_1=3.6 μT) was used to acquire CEST-weighted images from -7.2 to +7.2 ppm around the resonance of the ^{19}F atoms at the free 5F-BAPTA, which was assigned as 0 ppm. Saturation time (t_{sat}) was either 1500 ms to 2000 ms as indicated in the text.

^{19}F-iCEST of 500 nM of Ca^{2+}: An aqueous solution containing 0.5 mM of 5F-BAPTA and 500 nM in Hepes buffer (40 mM, pH=7.2) was transferred into a 20 mm NMR tube, which was located within a 25 mm NMR tube in order to centralize the sample in the coil for the MRI experiment. The same parameters used for ^{19}F-iCEST experiments were used except the followings: TR=3000 ms, RARE=8, FOV=6.0 cm (resolution=1.875×1.875 mm), and 168 averages

Magnetization Transfer Ratio (MTR) Images, iCEST images: The saturation transfer effect on the free 5F-BAPTA, i.e., the MTR or iCEST, was calculated for each voxel in the image by using a Lorentzian line shape fitting as previously described[1,2]. The mean MTR values were calculated from a ROI for each for each testing tube after B_0 correction for each voxel. Error bars represent the inter-voxel standard deviations in each sample.

Relaxation times: The same image geometry as in the ^{19}F-CEST experiments was used for the determination of T_1 and T_2 of the imaged samples. For T_1 measurements, a saturation recovery experiment was performed with TR values of 61, 214, 395, 615, 899, 1296 1964, and 4961 ms. A spin-echo experiment (TR=5000 ms) with multiple echoes was performed with variable echo times (TE=5, 10 15, 20, 25, 30, 35, and 40 ms) to determine the T_2 value of each sample.

Bloch equation simulations: Numerical solutions to the six Bloch equations including direct saturation of free 5F-BAPTA were obtained as described previously[3]. The relaxation parameters for ^{19}F used in the Bloch equations were $R_1 = 1/T_1$ with bound calcium (R_{1b}) = 0.71 s^{-1}, R_2 bound calcium (R_{2b})= 29 s^{-1}, whereas the R_1 and R_2 values of free 5F-BAPTA (R_{1f} and R_{2f}) were determined experimentally through inversion-recovery and saturation-recovery experiments as a function of pH on solutions containing 20 mM 5F-BAPTA as listed in Table S1.

iCEST Sensitivity: The validity of the ^{19}F-iCEST approach is based on the detectability of the free 5F-BAPTA with ^{19}F-MRI. As shown in Figure 4 (main text), 0.5 mM of 5F-BAPTA is detected at a lower spatial resolution compared to ^{1}H-MRI. iCEST images

overlaid on top of high resolution proton images will allow detailed spatial information to localize sources of iCEST signal. In addition, ^{19}F-MRI based approaches do not demand high ^{19}F signal-to-noise (SNR) due to the fact that any ^{19}F signal detected originates from the fluorinated compounds, as the endogenous ^{19}F content in biological tissues is negligible.[4] Additionally, by acquiring imaging at $+\Delta\omega$ and $-\Delta\omega$ (but not the whole Z-spectrum as used in this study), one could increase the number of averages and improve the SNR. Each image in the data set used for obtaining the Z-spectrum at Figure 4b was obtained in ~15 min. Therefore, by acquiring a dataset that consists of $+\Delta\omega$ and $-\Delta\omega$ images, one can obtain an iCEST effect from 500 nM Ca^{2+} (10% iCEST contrast) within 30 min with the experimental setup used (i.e, 0.5 mM of free 5F-BAPTA). Published results showed no toxic effect on cells when they were loaded with more than 1 mM of 5F-BAPTA[5]. Thus, our iCEST is a valid approach, in particular when these higher concentrations of 5F-BAPTA (1 mM) can be used to reduce the experimental scan time.

As an alternative, one may consider using the iCEST approach in a localized voxel-spectroscopy setup to improve SNR and reduce the acquisition time. This will allow the detection of even lower concentrations of the free 5F-BAPTA and [Ca^{2+}-5F-BAPTA, as shown before for 5-Fluoro-Uracil (5FU), which can be detected at micro-molar concentrations in vivo.[6]

In principle, the experimental acquisition parameters will determine the sensitivity of iCEST images.[4] This includes (i) the ^{19}F- agent T_1 and T_2 relaxation times which may be controlled by chemical probe design, (ii) improved image acquisition protocols such as SWIFT and UTE-based approaches adjusted to detect spins with short T_2, than used previously for saturation transfer imaging[7, 8], (iii) using MR scanners operating at high

magnetic field strengths, and (iv) RF-coil design, e.g., the use of multichannel RF coils or cryogenic RF coil technologies.

Figures

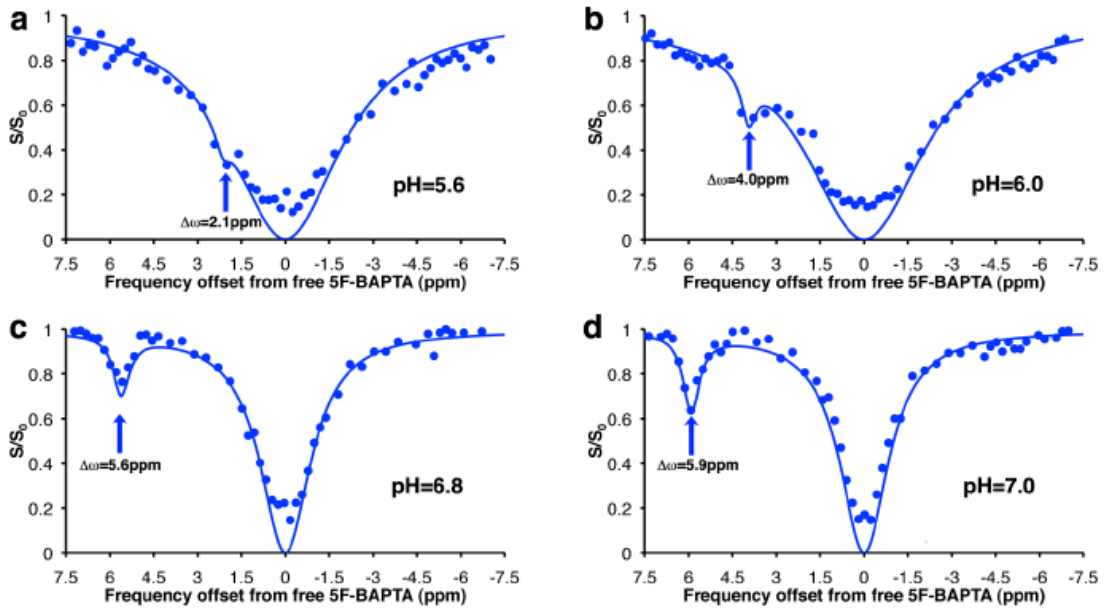

Figure S1. pH dependency of ^{19}F-CEST spectra of 5F-BAPTA: CEST-spectra of solutions containing 10 mM of 5F-BAPTA and 50 μM of Ca^{2+} in 40 mM Hepes buffer at solutions with the pH adjusted to a) 5.6, b) 6.0, c) 6.8, and d) 7.0. Solid lines represent Bloch simulations (two pool model) and arrows point to the Δω of the [Ca^{2+}-5F-BAPTA] complex. Note that the resolution and number of averages for the Z-spectra (experimental points) is lower for these samples compared to those used in Figure 2 (main text). The purpose of this experiment was to demonstrate that Δω could be determined from the Z-spectra. In addition, the SNR was low for this data, resulting in particularly poor quality measurements around saturation offsets of 0 ppm.

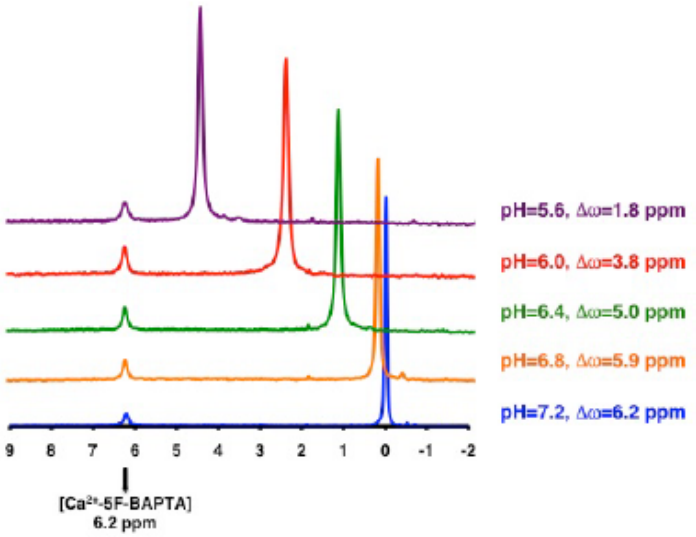

Figure S2. Chemical shift dependency of 5F-BAPTA as function of pH. ^{19}F-NMR spectra of solutions containing Ca^{2+}(0.5 mM), 5F-BAPTA (5 mM), and 5-Fluoro-Cytosine (5FC, 0.5 mM) as internal reference (set to -47 ppm) with 10% D_2O. The spectra were acquired at 470 MHz. The peak of 5-FC was calibrated at -47 ppm for convenience.

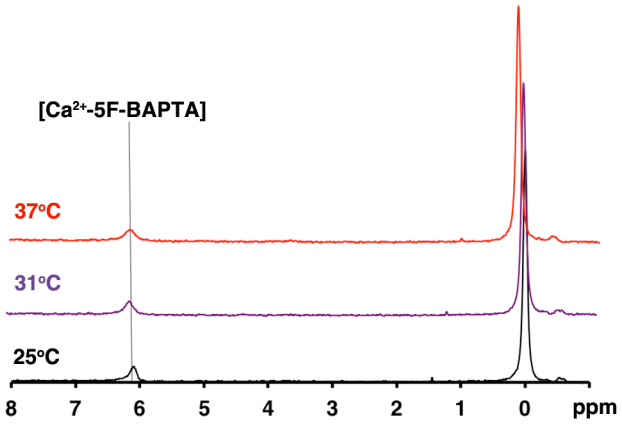

Figure S3. Effect of temperature on Δω. ^{19}F-NMR spectra of solutions containing Ca^{2+} (0.5 mM), 5F-BAPTA (5 mM), and 5-Fluoro-Cytosine (5FC, 0.5 mM) as internal reference (set to -47 ppm) in 10% D_2O. The spectra were acquired at 470 MHz. Increasing the temperature of the solution has no effect on the chemical shift offset of [Ca^{2+} -5F-BAPTA]. The resonance of the free 5F-BAPTA was found to be 0.0 ppm at 25°C, 0.12 ppm at 31°C, and 0.25 ppm at 37°C.

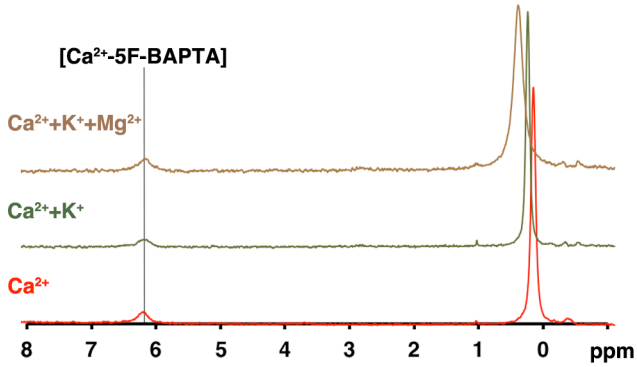

Figure S4. Effect of high concentration of fast exchanging ions (K^+ and Mg^{2+}) on Δω. ^{19}F-NMR spectra of solutions containing Ca^{2+}(0.5 mM), 5F-BAPTA (5 mM), and 5-Fluoro-Cytosine (5FC, 0.5 mM) as internal reference (set to -47 ppm) in 10% D_2O. The spectra were acquired at 470 MHz. Adding the fast exchanging ions K^+ (120 mM) and K^++Mg^{2+}(120 mM +1 mM) demonstrate a downfield shift in the resonance frequency of the free 5F-BAPTA at 0.32 ppm (for 120 mM K^+) and 0.48 ppm (for 120 mM of K^+ and 1 mM of Mg^{2+}). The temperature was set to 37°C and the peak of 5-FC was calibrated at -47 ppm for convenience.

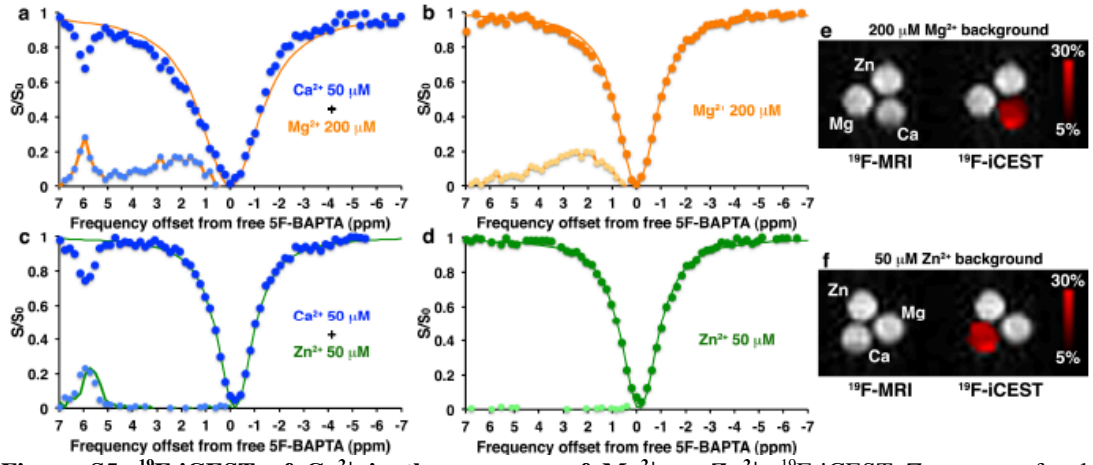

Figure S5. ^{19}F-iCEST of Ca^{2+} in the presence of Mg^{2+} or Zn^{2+}. ^{19}F-iCEST Z-spectra of solutions containing a) Ca^{2+} (50 μM) and Mg^{2+} (200 μM), b) Mg^{2+} (200 μM), c) Ca^{2+} (50 μM), and d) Zn^{2+} (50 μM) at pH=7.2, 37 °C, and 16.4 T. The MTR asymmetry (MTR_{asym}) plots of the background solutions are shown for 200 μM Mg^{2+} (a, b, light blue and light orange) and for 50 μM Zn^{2+} (c, d, light blue and light green). Solid lines represent Bloch simulations.

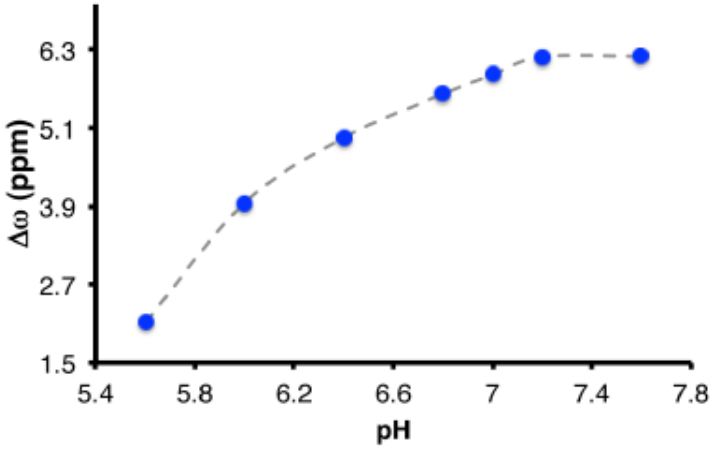

Figure S6. pH dependency of iCEST. The dependency of Δω between Ca^{2+}-bound and free 5F-BAPTA as obtained from iCEST Z-spectra. The phantom consisted of 8 mm NMR tubes containing 10 mM of 5F-BAPTA and 50 μM of M^{2+} in 40 mM Hepes buffer (pH=5.6-7.6). ^{19}F-iCEST data were acquired with B_1=3.6 μT/2000 ms at 37 ºC. The dependency of Δω between Ca^{2+}-bound and free 5F-BAPTA was obtained from ^{19}F-iCEST Z-spectra

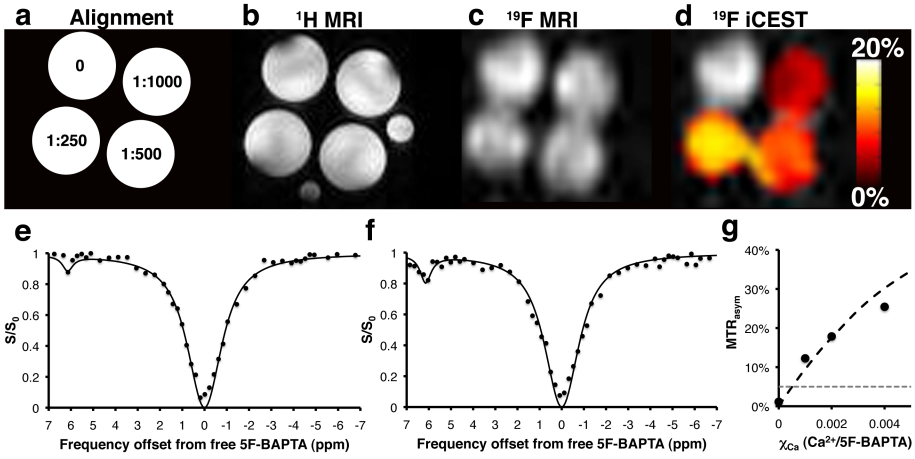

Figure S7. Sensing Ca^{2+} using iCEST. a) Alignment of four tubes containing 5 mM of 5F-BAPTA (pH=7.2) and different molar fractions (χ_{Ca} =1:250, 1:500, 1:1000, 1:0) between Ca^{2+} and 5F-BAPTA for the phantom (pH=7.2, 16.4 T, 37ºC). b) ^{1}H-MR image. Small water tubes (shown on ^{1}H-MRI) were included to determine the orientation of the samples. c) ^{19}F-MR image, and d) overlay of ^{19}F-iCEST image (Δω=6.2 ppm) on ^{19}F-image. iCEST Z-spectra for a tube with e) χ_{Ca}=1:1000 and f) χ_{Ca}=1:500 samples. Solid lines represent Bloch simulations. g) Plot of χ_{Ca} vs. MTR_{asym} for iCEST data acquired at B_1=3.6 μT, t_{sat}=1.5 s. A 5% threshold is shown as a gray dashed line, which is reached at χ_{Ca}= 1:2000.

Table S1. $\Delta\omega$ and T_2 dependency on pH

pH	$\Delta\omega$ (ppm)	T_2 (ms)	T_1 (ms)
5.6	2.1	6[a]	715
6.0	4.0	10	715
6.4	5.0	11	715
6.8	5.6	25	715
7.0	5.9	32	715
7.2	6.2	38	715
7.6	6.2	N.D	715

[a] Estimated from the Bloch equation fitting
N.D. = Not Determined

References

(1) Jones, C. K.; Polders, D.; Hua, J.; Zhu, H.; Hoogduin, H. J.; Zhou, J.; Luijten, P.; van Zijl, P. C. *Magn Reson Med* **2012**, *67*, 1579.
(2) Liu, G.; Li, Y.; Sheth, V. R.; Pagel, M. D. *Mol Imag* **2012**, *11*, 47.
(3) McMahon, M. T.; Gilad, A. A.; Zhou, J.; Sun, P. Z.; Bulte, J. W. M.; van Zijl, P. C. M. *Magn Reson in Med* **2006**, *55*, 836.
(4) Ahrens, E. T.; Zhong, J. *NMR Biomed* **2013**. doi: 10.1002/nbm.2948
(5) Smith, G. A.; Hesketh, R. T.; Metcalfe, J. C.; Feeney, J.; Morris, P. G. *Proc Natl Acad Sci U S A* **1983**, *80*, 7178.
(6) Martino, R.; Gilard, V.; Desmoulin, F.; Malet-Martino, M. *J Pharm Biomed Anal* **2005**, *38*, 871
(7) Soesbe, T. C.; Togao, O.; Takahashi, M.; Sherry, A. D. *Magn Reson Med* **2012**, *68*, 816.
(8) Du, J.; Takahashi, A. M.; Bydder, M.; Chung, C. B.; Bydder, G. M. *Magn Reson Med* **2009**, *62*, 527.